Electromigration of substitutional impurities in metals: Theory and application in Al and Cu

Dekker, J.P.; Lodder, A.; van Ek, J.

published in
Physical Review B. Condensed Matter
1995

document version
Publisher's PDF, also known as Version of record

Electromigration of substitutional impurities in metals: Theory and application in Al and Cu

J. van Ek*
Department of Chemistry and Materials Science, L-268, Lawrence Livermore National Laboratory, P.O. Box 808, Livermore, California 94551

J.P. Dekker and A. Lodder
Faculteit der Natuurkunde en Sterrenkunde, Vrije Universiteit, de Boelelaan 1081, 1081 HV Amsterdam, The Netherlands
(Received 30 March 1995)

A theory describing scattering of Bloch electrons by an atom halfway along its path towards a neighboring vacancy is cast in a computationally convenient form. This allows for the computation of the electromigration wind force at the saddle-point position in an elementary diffusion step, where the cross section for Bloch electron-impurity scattering of the migrating ion is at a maximum. Results for atoms migrating into a neighboring vacancy in Al and Cu are presented. The outcome is found to be consistent with experimental information, even though only a two-atom cluster was embedded in the host metal. It is concluded that even more realistic calculations of the electromigration wind force on substitutional impurities in metals are possible upon incorporation of the effects of local lattice deformation and charge transfer.

I. INTRODUCTION

The phenomenon whereby an electric field induces macroscopic atomic currents in condensed matter is known as electromigration. Random diffusive motion of interstitial or substitutional impurities is directed through a driving force $\vec{F}$. It has become common to distinguish two contributions to $\vec{F}$, namely, (1) the direct force, $\vec{F}_{\rm direct}$, resulting from the direct electrostatic interaction of the electric field with a possible net charge on the impurity; and (2) the so-called wind force, $\vec{F}_{\rm wind}$, resulting from electron-impurity scattering of the current carrying electrons. In isotropic systems, each of these forces is characterized by a proportionality factor describing the susceptibility to the applied electric field: the effective valence, Z^*, for the driving force, the direct valence, $Z_{\rm direct}$, for the direct force, and the wind valence, $Z_{\rm wind}$, for the wind force. Thus,

$$\vec{F} = Z^* e\,\vec{E} = \vec{F}_{\rm direct} + \vec{F}_{\rm wind} = (Z_{\rm direct} + Z_{\rm wind}) e\,\vec{E}\ , \tag{1.1}$$

where $\vec{E}$ is the electric field and e is the elementary charge.

Combined experimental and theoretical effort has resulted in substantial progress in understanding electromigration of hydrogen in metals over the past decade (see Ref. 1 and references therein). Superficially one may argue that the case where atoms move from lattice site to lattice site by a vacancy mechanism should be no more difficult. However, from a theoretical point of view, the description of the electronic structure for a migrating substitutional atom imposes additional difficulties. Interstitially dissolved hydrogen diffuses through a crystal with metal atoms associated with each lattice site. For substitutional electromigration, the situation is fundamentally different. At the saddle-point position half-way along the path towards a neighboring vacancy, reference to the perfect lattice is no longer meaningful, and the concept of embedding an impurity cluster of quite general shape must be invoked. Experiments on migration of substitutional defects have to be carried out at high temperatures and/or high current densities so that the mobility of the migrating species is sufficiently large to allow for the detection of concentration variations, due to electromigration within a reasonable time frame. In dilute binary alloys, the reduction of experimentally determined so-called *apparent* effective valences to regular effective valences Z^* is complicated by correlation effects between the vacancy and solute fluxes in the sample (see, for instance, Refs. 2 and 3). For self-electromigration, the interpretation of the experimentally determined atomic flux is more straightforward. Huntington[2] compiled data on Z^* for some twenty metals.

Theoretical results for electromigration in pure metals can be directly verified by empirical results. Once agreement between experiments in pure metals and results from the approach outlined in this paper is shown, an attractive approach to the resolution of correlation effects between atomic currents in dilute alloys emerges. Calculated valences for solvent and solute should be compared with experimental apparent effective valences, and the coefficients relating the apparent and regular effective valence can be deduced. Interesting cross checks with earlier results from the kinetic analysis of solute effects[3] become feasible.

In the semiconductor industry, where electromigration induced failure of metallic (Al) interconnects still forms a major problem, the low diffusivity of substitutional de-

0163-1829/95/52(12)/8794(7)/$06.00

fects under operating conditions has led to so-called accelerated testing (i.e., at elevated temperature and increased current density). As it turns out, results of these tests are not always transferable to operating conditions. It is, for instance, unclear how the ratio of electromigration induced mass transport at grain boundaries and in the bulk is affected upon raising temperature. This is an important example of a situation where the fundamental understanding of the physics underlying electromigration will prove to be useful.

So far, few efforts to calculate the wind force in dilute alloys have been reported on. Finite cluster calculations for model potentials[4] and for Nb based alloys[5] revealed that it is unnecessary to invoke "hole-impurity scattering," as opposed to electron-impurity scattering, in order to account for positive wind valences. Quantitatively the results of such calculations rather strongly depend on the size of the cluster. Gupta *et al.*[6] performed calculations in noble metals and Nb, neglecting multiple scattering in the alloy. Later it was shown that this is an unjustified approximation.[7] Results of pseudo (model) potential calculations for a wide variety of systems have been reported by Sorbello.[8] Although the first in their kind, the above-mentioned studies have in common that they lack proper account of typical solid state features or that the method used cannot be applied to transition metals.

A complete theory for the electromigration wind force in dilute alloys was formulated some ten years ago[9] (to be referred to as I) within the Korringa-Kohn-Rostoker (KKR) Green function approach. For atoms moving from one lattice site into a vacant neighboring site during an elementary jump in the migration process, one easily envisages the position at which the migrating ion is halfway along the migration path (the saddle-point position). The cross section for scattering of Bloch electrons by the migrating species will be large at the saddle point, and consequently the wind force will be large in magnitude. In addition, lattice deformation of the surrounding atoms can be quite large. This requires a treatment of the electronic structure of an impurity *cluster* of rather general shape, embedded in an otherwise perfect crystal. The philosophy behind the treatment given in I is to replace a suitable cluster of host atoms with the impurity cluster. Instead of the perfect crystal, the metal containing the void will serve as a reference system in the Green function approach. Within the framework of multiple scattering by a collection of muffin-tin potentials, an exact expression for the alloy (scattering) wave function was derived in I, in part based on earlier experience.[10] Matrix elements of a force operator with respect to the alloy wave function can be evaluated, yielding the wind force in terms of impurity phase shifts, cluster t matrices and alloy wave function coefficients. The alloy wave function coefficients, in turn, involve the evaluation of Brillouin-zone integrals with highly singular integrands.

At the time, when I was published, it was unclear from a practical point of view how to go about actually calculating the wind force on atoms in such a complicated impurity cluster. It was decided that the special case of an interstitial impurity with the accompanying perturbation of its local environment was more attractive as a starting point for further research. The approach described in I, but applied to interstitial impurities has proven successful in the theoretical investigation of de Haas–van Alphen quantities (Dingle temperatures and cross-sectional area changes),[11] electromigration of hydrogen in metals[12,13] and hydrogen induced resistivity.[13,14] This reinforced the belief that it is worthwhile to develop computer codes that evaluate the relevant quantities for the more general case of oblong impurity clusters typically met in substitutional electromigration. In this paper, a convenient computational scheme for the evaluation of Bloch electron scattering by such impurity clusters, hitherto considered unsuitable for any theoretical calculation, is developed on the basis of expressions given in I.

The paper is organized as follows. In Sec. II, a reformulation of the formalism first described in I is presented. Alternative expressions for the relevant multiple scattering quantities in the original work I by Lodder allow for efficient implementation of the formalism on a digital computer. Proof of principle is established in Sec. III, where first results of electromigration wind force calculations in Al and Cu are presented. In these examples, typical for electromigration, *all* multiple scattering effects for a migrating atom at the saddle-point position are exactly accounted for. A less complicated case, where the migrating ion is at its initial position next to a vacancy, is of special interest in that present results should match those earlier obtained from a more conventional but limited approach.[7] The wind force acting on a migrating ion is found to be at maximum halfway along the migration path, where the perturbation with respect to the fcc host lattice is largest. This stipulates the fact that, in order to perform realistic calculations on substitutional electromigration, one really has to evaluate the multiple scattering of Bloch electrons at the saddle-point position. Section IV summarizes the present work.

II. COMPUTATIONALLY CONVENIENT FORMULATION

The starting point will be expression (21) of I for the wind force on an impurity atom in a dilute alloy, represented by a collection of muffin-tin potentials,

$$\vec{F}_{\text{wind}} = 2eE\tau \sum_{L} \sum_{\tilde{m}=-l-1}^{l+1} (\cot \eta_{1l+1} - \cot \eta_{1l})\, \vec{D}_{L,l+1,\tilde{m}} \times \sum_{p'L'p''L''} \text{Re}\{T^{*}_{1,l+1,\tilde{m},p'L'} T_{1Lp''L''} \times \vec{V}_{p'L'p''L''} \cdot \hat{E}\} \,. \tag{2.1}$$

Although expression (2.1) was derived with an impurity cluster embedded in an fcc or bcc metal in mind, it can easily be extended to include more complex host lattices. Since the aim is to calculate the wind force $\vec{F}_{\text{wind}}$ on specific defect atoms, Eq. (2.1) will be analyzed step by step, and a convenient formulation for various elements in Eq. (2.1) will be given. In Eq. (2.1) and in the following, labels p and j (or j_c) refer to atomic positions in

the impurity or host cluster, respectively, while n can be either of the two. Lattice positions in the perfect crystal are labeled with j_h, while the migrating ion carries the label "1."

The transport relaxation time in the isotropic approximation, τ, enters as a semi-empirical parameter, to be determined from tabulated experimental bulk resistivities for the host metal at the appropriate temperature.[6,7] An externally applied electric field $\vec{E}$ (magnitude E, direction $\hat{E} = \frac{\vec{E}}{E}$) generates a current density in the sample, which in turn induces the wind force on the migrating species. The magnitude and direction of $\vec{F}_{\text{wind}}$ strongly depend on the details of the alloy wave function in the vicinity of the migrating atom. Scattering properties of the muffin potentials are described by the phase shifts η_{1l}, where the subscript "1" labels the moving atom. Real spherical harmonics are used throughout, and angular momentum l and the label m, indicating spatial orientation, are combined in $L \equiv (l, m)$ as much as possible. Cluster t matrices, T, describe multiple scattering within the impurity cluster and can be readily evaluated (see Appendix). The vectorial matrix $\vec{D}_{LL'}$ is closely related to Gaunt coefficients.[15]

The central quantity in Eq. (2.1) is the matrix,

$$\tau\vec{V}_{pLp'L'} \equiv \sum_{n\vec{k}} \tau_{n\vec{k}} a^*_{n\vec{k},pL} \vec{v}_{n\vec{k}} a_{n\vec{k},p'L'} \frac{\partial f_0}{\partial \epsilon_{n\vec{k}}} . \tag{2.2}$$

In this definition of $\tau\vec{V}$, the relaxation time approximation has been adopted, implying that the electron mean free path is written as $\tau_{n\vec{k}}\vec{v}_{n\vec{k}}$ ($\vec{v}_{n\vec{k}}$ the group velocity), so that full anisotropy for the transport relaxation time is retained. In practice, only part of the anisotropy is retained through $\vec{v}_{n\vec{k}}$, while $\tau_{n\vec{k}}$ is replaced by an average value τ. This has proven to be a successful approach in the study of metal-hydrogen systems.[12] At sufficiently low temperature the energy derivative of the Fermi-Dirac equilibrium distribution function for the electrons, $\frac{\partial f_0}{\partial \epsilon_{n\vec{k}}}$, is strongly peaked and only scattering states at energies close to the Fermi energy ($\epsilon_{n\vec{k}} \simeq \epsilon_F$) contribute to the matrix element in Eq. (2.2).

For impurity clusters with atoms at positions that greatly differ from lattice sites, the usual KKR-ansatz for the alloy wave function

$$\Psi_{n\vec{k}}(\vec{x} + \vec{R}_p) = \sum_L R_{pL}(\vec{x}) c_{n\vec{k},pL} \tag{2.3}$$

is inappropriate. Instead, a form that expresses the embedment of the impurity cluster in the host crystal must be used

$$\Psi_{n\vec{k}}(\vec{x} + \vec{R}_p) = \sum_L R_{pL}(\vec{x})\, t_{pl}^{-1} \sum_{p'L'} T_{pLp'L'}\, a_{n\vec{k},p'L'}, \tag{2.4}$$

where t_{pl} are single-site t matrices for atoms in the impurity cluster. Alloy wave function coefficients $a_{n\vec{k}}$ can be shown to relate to host coefficients $a^h_{n\vec{k}}$ as

$$\sum_{p'L'p''L''} \left(\delta_{pp''}\delta_{LL''} + T^{\text{back}}_{pLp'L'} T_{p'L'p''L''}\right) a_{n\vec{k},p''L''} = \sum_{j'L'j''L''} \left(\delta_{pj''}\delta_{LL''} + T^{\text{back}}_{pLj'L'} T^h_{j'L'j''L''}\right) a^h_{n\vec{k},j''L''} . \tag{2.5}$$

The coefficients $a^h_{n\vec{k}}$ are trivially related to the usual KKR wave function coefficients $c^h_{n\vec{k}}$ through

$$a^h_{n\vec{k},jL} = \sum_{j'L'} T^{h\,-1}_{jLj'L'} t^h_l c^h_{n\vec{k},j'L'} , \tag{2.6}$$

in which T^h is a cluster t matrix for the collection of host atoms to be replaced with the alloy cluster, and t^h_l are the single-site t matrices for the metallic host. T^{back} describes the backscattering from the crystalline environment of the embedded cluster, and, according to Eq. (2.5), has to be known with respect to both host and alloy positions in the cluster. Computation of T^{back} involves Brillouin-zone integrals $\mathcal{T}_{nLn'L'}$, with integrands that are highly singular at both the Fermi surface and the free electron sphere. These integrals will be discussed later. Once the $\mathcal{T}_{nLn'L'}$ are available, the $T^{\text{back}}_{nLn'L'}$ can be obtained from the following sequence of matrix manipulations (angular momentum indices often suppressed)

$$\begin{aligned} T^{\text{back}}_{jj'} &= \textstyle\sum_{j''} \mathcal{T}_{jj''} \left(1 - T^h\mathcal{T}\right)^{-1}_{j''j'} , \\ T^{\text{back}}_{pj} &= \mathcal{T}_{pj} + \textstyle\sum_{j''j'''} \mathcal{T}_{pj''} T^h_{j''j'''} T^{\text{back}}_{j'''j'} , \\ T^{\text{back}}_{jLpL'} &= T^{\text{back}}_{pL'jL} , \\ T^{\text{back}}_{pp'} &= \mathcal{T}_{pp'} + \textstyle\sum_{jj'} \mathcal{T}_{pj} T^h_{jj'} T^{\text{back}}_{j'p'} . \end{aligned} \tag{2.7}$$

After substitution of Eqs. (2.6) and (2.5) in Eq. (2.2) and the introduction of

$$Z_{pLp'L'} = \delta_{pp'}\delta_{LL'} + \sum_{p''L''} T^{\text{back}}_{pLp''L''} T_{p''L''p'L'} \tag{2.8}$$

and

$$X_{pLj'L'} = \left(T^{\text{back}}_{pLj'L'} - B^{pj'}_{LL'}\right) t^h_{l'}, \tag{2.9}$$

with $B^{nn'}_{LL'}$ the well-known free space structural Green function matrix given by Eq. (A3) in the Appendix, the wave function coefficients are written as

$$a_{n\vec{k},pL} = \sum_{p'L'} Z^{-1}_{pLp'L'} \left(c^h_{n\vec{k},p'L'} + \sum_{j''L''} X_{p'L'j''L''} c^h_{n\vec{k},j''L''} \right) . \tag{2.10}$$

Upon substitution of Eq. (2.10) in Eq. (2.2), one arrives at an expression for $\vec{V}$ that only involves KKR host wave function coefficients $c^h_{n\vec{k},nL}$,

$$\vec{V}_{pLp'L'} = \sum_{p_1L_1,p_2L_2,j_3L_3,j_4L_4} \left(Z^{-1}_{pLp_1L_1}X_{p_1L_1j_3L_3}\right)^* \vec{I}_{j_3L_3j_4L_4} \left(Z^{-1}_{p'L'p_2L_2}X_{p_2L_2j_4L_4}\right) + \sum_{p_1L_1,p_2L_2,j_3L_3} \left(Z^{-1}_{pLp_1L_1}\right)^* \vec{I}_{p_1L_1j_3L_3} \left(Z^{-1}_{p'L'p_2L_2}X^{-1}_{p_2L_2j_3L_3}\right) + \text{H.c.} + \sum_{p_1L_1,p_2L_2} \left(Z^{-1}_{pLp_1L_1}\right)^* \vec{I}_{p_1L_1p_2L_2} \left(Z^{-1}_{p'L'p_2L_2}\right) , \tag{2.11}$$

with

$$\vec{I}_{nLn'L'} = \sum_{n\vec{k}} c^{h*}_{n\vec{k},nL}\vec{v}_{n\vec{k}}c^{h}_{n\vec{k},n'L'}\frac{\partial f_0}{\partial \epsilon_{n\vec{k}}} . \tag{2.12}$$

At temperatures where the energy derivative of the Fermi-Dirac distribution function still is strongly peaked at the Fermi energy ($\frac{\partial f_0}{\partial \epsilon_{n\vec{k}}} \simeq -\delta(\epsilon_{n\vec{k}} - \epsilon_F)$), the summation can be replaced by an integral over the Fermi surface of the metal under consideration. As was shown previously,[16,17] the coefficients $c^h_{n\vec{k},nL}$ in Eq. (2.12) can readily be determined from KKR eigenvectors and eigenvalues, and structural matrices with respect to site $\vec{R}_n$.

Still to be discussed are the Brillouin-zone integrals that enter the construction of the backscattering t matrix, T^{back}, through Eq. (2.7),

$$\mathcal{T}_{nLn'L'} = \frac{1}{V_{\text{BZ}}}\int^{\text{BZ}} d^3k \left(\bar{b}^n(\vec{k})\, M^{-1}(\vec{k})\, \bar{b}^{n't}(-\vec{k})\right)_{LL'} \times e^{i\vec{k}\cdot(\vec{R}_n - \vec{R}_{n'})} . \tag{2.13}$$

$M(\vec{k}) = -t^{h^{-1}} + b(\vec{k})$ is the KKR matrix at a particular energy and k point, and is given in terms of the single-site host t matrix. A superscript "t" denotes transposition of a matrix. The Fourier transformed structural Green function $b(\vec{k}) \equiv b^{j_h}(\vec{k})$ is defined as

$$b^n_{LL'}(\vec{k}) = \sum_{j_h} B^{nj_h}_{LL'}\, e^{-i\vec{k}\cdot(\vec{R}_n - \vec{R}_{j_h})} , \tag{2.14}$$

and overlined structure matrices are defined as

$$\bar{b}^n_{LL'}(\vec{k}) = b^n_{LL'}(\vec{k}) - \sum_{j_c} B^{nj_c}_{LL'}\, e^{-i\vec{k}\cdot(\vec{R}_n - \vec{R}_{j_c})} . \tag{2.15}$$

Index j_c runs over the sites in the cluster that had to be "removed" from the metallic host in order to make room for the impurity cluster. Since $M(\vec{k})$ and $\bar{b}^n(\vec{k})$ have poles at $\epsilon = (\vec{k} + \vec{g})^2$ ($\vec{g}$ a reciprocal lattice vector), the integrand as a whole diverges at the free electron sphere. In addition, the inverse KKR matrix is singular at constant energy surfaces defined by the KKR determinantal condition $\det(M(\vec{k})) = 0$. Recently, a very elegant and efficient method that entirely eliminates the free electron poles has become available.[18] Numerical convergence of the (principal value) integral with respect to the divergence of $M^{-1}(\vec{k})$ has already been shown by Coleridge *et al.*[19]

It is interesting to note that the embedded cluster formalism, when applied to a single-site impurity, involves Brillouin-zone integrals that are singular only at constant energy surfaces of the dispersion relation. Realizing that for the single-site case $\bar{b}^n(\vec{k}) \to b(\vec{k})$ and $\int^{\text{BZ}} d^3k\, b(\vec{k}) = 0$, it is seen that

$$t^h\mathcal{T}_{jj}t^h = t^h\left[\frac{1}{V_{\text{BZ}}}\int^{\text{BZ}} d^3k\, b(\vec{k})M^{-1}(\vec{k})\, b^t(-\vec{k})\right]t^h = t^h + \frac{1}{V_{\text{BZ}}}\int^{\text{BZ}} d^3k\, M^{-1}(\vec{k}) . \tag{2.16}$$

Addition of a phase factor that causes the integrand to oscillate results in an equality that will prove very useful for testing purposes,

$$t^h\left[\frac{1}{V_{\text{BZ}}}\int^{\text{BZ}} d^3k\, b(\vec{k})\, M^{-1}(\vec{k})\, b^t(-\vec{k})\, e^{i\vec{k}\cdot\vec{R}_{jj'}}\right]t^h = t^h\delta_{jj'} + t^hB^{jj'}t^h + \frac{1}{V_{\text{BZ}}}\int^{\text{BZ}} d^3k\, M^{-1}(\vec{k})\, e^{i\vec{k}\cdot\vec{R}_{jj'}} . \tag{2.17}$$

The single-site case is represented by $j = j'$, while the $j \neq j'$ integral probes the sensitivity to the oscillatory exponential factor. This relation offers an interesting check on the treatment of the free electron poles proposed in Ref. 18, since the integrand on the left hand side of Eq. (2.17) still is singular at $\epsilon = (\vec{k} + \vec{g})^2$, while $M^{-1}(\vec{k})$ is not. Numerical results on the extent to which Eq. (2.17) is satisfied will be given in the next section, along with first results for an elementary cluster relevant to electromigration.

III. RESULTS ON ELECTROMIGRATION IN Al AND Cu

Simplest, yet relevant to electromigration, is the cluster consisting of two lattice sites: the migrating atom and a neighboring vacancy (see Fig. 1). The impurity cluster to be embedded in the metalic host consists of (1) an atom and a vacancy at lattice sites or (2) just the migrating ion at the saddle-point position halfway along the migration path. In reality, local lattice deformation as well as charge transfer may be considerable and the effect on the wind force will be evaluated in forthcoming, more elaborate calculations. The objective of the present calculations is to establish proof of principle.

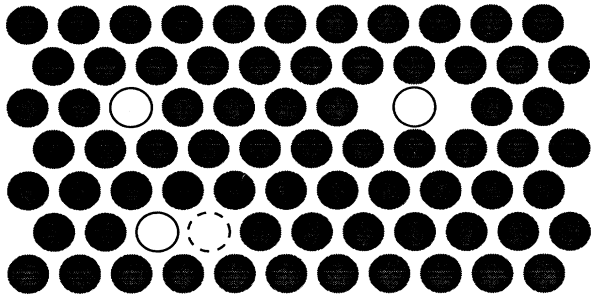

FIG. 1. The simplest cluster that can be used in the calculation of the electromigration wind force at the saddle-point position halfway along the migration path. A host cluster of two atoms had to be removed in order to allow for embedding of (lower left) the migrating atom and a vacancy, both at lattice sites or (upper right) the single migrating ion at the saddle-point position. Also shown (upper left) is a single site impurity.

Since there is considerable interest in electromigration of Al and Cu in Al metal and because the Fermi surface of Al is not entirely trivial, these systems, along with Al and Cu in Cu metal are investigated here. First of all, the accuracy with which the Brillouin zone and Fermi surface integrals are computed will be discussed. For host lattice sites j and j' equality (2.17) can be used as a criterion. As mentioned in Sec. II, the integrand on the left hand side contains two kinds of singularities. The divergent character of both b and M at the free electron sphere, as well as the singularity of M^{-1} at the Fermi surface prompt for special care in the principal value integration of $b\,M^{-1}b$.

The integral over $b\,M^{-1}b$ is evaluated by subtracting and adding a term $f^{\mathrm{FES}}(\vec{k})$ that precisely cancels the singular behavior of the integrand at the free electron sphere (FES),

$$b(\vec{k})\,M^{-1}(\vec{k})\,b^t(-\vec{k}) = \left\{b(\vec{k})\,M^{-1}(\vec{k})\,b^t(-\vec{k}) - f^{\mathrm{FES}}(\vec{k})\right\} + f^{\mathrm{FES}}(\vec{k}). \tag{3.1}$$

This term is chosen such that it can be analytically integrated over the Brillouin zone, and the result is then simply added. Numerical integration of the expression between curly brackets no longer suffers from poles at the free electron surface. A convenient choice for $f^{\mathrm{FES}}(\vec{k})$ is proposed in Ref. 18. Equation (2.17) provides a measure of the degree of convergence reached through comparison of the $b\,M^{-1}b$ integral, treated as outlined above, with well-established integrals of M^{-1}.[19]

For host lattice positions only, the free electron singularity can be entirely isolated in $b(\vec{k})\,e^{i\vec{k}\cdot\vec{R}_{jj'}}$. Integration yields the term proportional to $B^{jj'}$ in Eq. (2.17). This provides an additional test of the numerical accuracy through integration of $(b\,M^{-1}b-b)\,e^{i\vec{k}\cdot\vec{R}_{jj'}}$, which should equal the right hand side of Eq. (2.17) minus $t^h B^{jj'} t^h$.

For Cu and Al metal, elimination of the free electron poles from $bM^{-1}b$ through either $f^{\mathrm{FES}}(\vec{k})$ or $b(\vec{k})$ resulted in errors of less than 1%, with respect to the right hand side of Eq. (2.17). Integrated matrix elements for angular momenta up to $l_{\max} = l'_{\max} = 3$ were evaluated, and the conclusion is that the free electron poles are integrated to a sufficient degree of accuracy.

Besides the integral in Eq. (2.13), the formalism also contains Fermi surface integrals (2.12), arising from the matrix elements of the force operator. These integrals can be tested independently upon realizing that an unperturbed host atom in the crystal does not scatter Bloch electrons. This implies a vanishing wind force on such an atom. From Eq. (2.5), it is seen that for this situation the alloy wave function coefficients reduce to host wave function coefficients. Any inaccuracies in T^{back} are canceled through the appearance of $T^{\mathrm{back}}T^h$ on both sides of Eq. (2.5). If the wind force, Eq. (2.1), does not vanish, this must be due to imprecise evaluation of the Fermi surface integrals Eq. (2.12). Performing this test for pure Cu and Al and comparing the resulting wind forces with the force on Al in Cu and Cu in Al metal, respectively, the wind force on the host atom is found to be more than three orders of magnitude smaller. The Fermi surface integrals are evaluated to a sufficient degree of accuracy.

Application of the computational scheme described in the previous section leads to position dependent 3×3 wind valence tensors $\underline{Z}_{\mathrm{wind}}(\vec{R}_1)$ related to the wind force as

$$\vec{F}_{\mathrm{wind}} = \underline{Z}_{\mathrm{wind}}(\vec{R}_1)\,e\,\vec{E}\ , \tag{3.2}$$

where $\vec{R}_1$ is the position of the migrating atom. Since only the component of the wind force along the migration path (in Al and Cu an fcc [110] direction) is of immediate interest, the tensor reduces to a scalar. Spherically symmetric muffin-tin potentials and corresponding phase shifts for the host metal and the impurity cluster were derived from overlapping charge densities as described in Ref. 7. The angular momentum cutoff was taken at $l_{\max} = 3$. Accounting for charge neutrality through a generalized Friedel-sum rule is known to modify Z_{wind}, but was neglected here. Results for the scalar wind valence on migrating atoms in Al and Cu are given in Table I. Only the initial configuration (atom and vacancy at neighboring lattice sites) and the saddle-point configuration are considered, but, in principle, more points along the path can be sampled. Values for the transport relaxation time are the same as those used in Ref. 7 ($\tau = 42$ Ry atomic units for Al and $\tau = 130$ for Cu).

A look at the total wind valence (bold type in Table I) shows that, without exception, the wind force is at maximum magnitude at the saddle-point position (s). Comparing with the initial position (i), $|Z_{\mathrm{wind}}|$ is increased by a factor of 1.3 (Al in Cu metal) to more than an order of magnitude (Cu in Cu metal). Such a tendency was to be expected on intuitive grounds. Here, for the first time, this is explicitly demonstrated in a realistic model of the metal-impurity-vacancy system that accounts for all multiple scattering effects at both the initial and the

TABLE I. Wind valence in Al and Cu. Partial l, $l+1$ contributions to Z_{wind} as well as total Z_{wind} at the initial (i) and saddle-point (s) position. Estimates for the transport relaxation time in Al ($\tau = 42$, in Rydberg atomic units) and Cu ($\tau = 130$) were taken from Ref. 7.

Host	Partial wave	Al atom		Cu atom	
	$l, l+1$	i	s	i	s
Al	s-p	0.02	0.62	-0.74	0.80
	p-d	-2.13	-18.5	-2.20	-11.8
	d-f	-0.11	-0.82	-7.16	-6.39
	total	**-2.22**	**-18.7**	**-10.1**	**-17.4**
	Ref. 7	-2.38		-10.7	
Cu	s-p	0.24	-0.16	1.13	-0.16
	p-d	-5.47	-7.54	-0.47	-1.43
	d-f	-0.46	0.41	0.42	-11.6
	total	**-5.69**	**-7.29**	**1.09**	**-13.9**
	Ref. 7			1.05	

saddle-point position. Interestingly, a change in sign of the wind force on Cu in Cu metal is observed as the Cu atom moves towards the saddle point. From the interpretation of calculated wind valences for hydrogen in Nb and Ta,[12] it is known that such a change of sign is the result of a reversal of the field induced dipolar charge distribution around the migrating ion. For substitutional electromigration the presence of a vacant site next to the migrating species may give rise to additional effects on the field induced charge distribution.

From Table I, it is seen that the dominant contribution to the wind force on an Al atom in Al or Cu metal is due to coupling between the p and the d channel [(l and $l+1$ in Eq. (2.1)], both at the initial and saddle-point position. For Cu in Al metal both p-d and d-f contribute significantly, suggesting a relation with the introduction of d-scattering strength on the Cu atom. Realizing that in the free electron model the wind force reduces to

$$\vec{F}_{\text{wind}} = -e\vec{E}\tau\frac{4\,\epsilon_F}{3\,\pi\,m}\sum_l (l+1)\sin^2(\eta_{l+1}-\eta_l)\ , \quad (3.3)$$

with m the electron rest mass and η_l the phase shifts of the migrating atom (see for instance I), the partial contributions to the wind valence in Al metal can be rationalized. Since Al is a nearly free electron metal with similar and dominant $l = 0$ and $l = 1$ phase shifts, Eq. (3.3) should be of some relevance. Based on the free electron result for the wind force the s-p contribution to Z_{wind} on an Al atom is expected to be small, but p-d coupling will be significantly larger (small η_2 for Al). Similarly, a d-scatterer such as Cu, will experience a wind force through coupling of the d with p and f channels. This free electron picture qualitatively explains the results quoted for Al metal in Table I.

For Cu, at the initial position in the transition metal Cu, the positive s-p contribution survives due to the cancellation of p-d and d-f. Here, as for Al in Al metal, any wind force on the Cu atom is induced by multiple scattering effects, due to the presence of the vacancy. Multiple scattering manifests itself in the s-p channel for Cu in Cu, while for Al in Al, the p-d channel is seen to be most important. At the saddle-point d-f coupling is strongly dominant, indicating that the Cu impurity behaves as an "interstitial" with a large d-scattering cross section.

TABLE II. Experimental effective valence, Z^*, and path-averaged wind valence in Al and Cu.

System	Experimental Z^*	Calculated Z_{wind}
Al in Al	-16.4	-10.5
Cu in Al	-6.8	-13.8
Cu in Cu	-4.1	-6.4
Al in Cu		-6.5

The lines in Table I labeled with "Ref. 7" give values of Z_{wind} at the initial position as calculated with the conventional method that cannot treat the saddle-point position. These values are within a few percent of the wind valences calculated according to the different method presented in this paper.

In Table II, the experimental value for the effective valence, Z^*, of Cu in Al was taken from,[3] while Z^* for self-electromigration of Al and Cu are taken to be the average of data from Huntington's review paper.[2] Experimental values for Z^* quoted in the present study are the same ones as were used in Ref. 7. These numbers are to be compared with the average of calculated wind valences along the path. Since two different points along the path are considered, the average of the initial and the saddle-point value was taken. It is not the intent to make a detailed comparison, since the calculations do not account for the effects of charge transfer and local lattice deformation. Especially at the saddle-point lattice deformation will be substantial. In addition, there may very well be a contribution from the direct force to the Z^* values quoted. According to the Bosvieux-Friedel model for the direct force,[20] it is estimated that $Z_{\text{direct}} = \frac{1}{2}Z_{\text{host}} = 1.5$ for impurities in Al and $Z_{\text{direct}} = 0.5$ for impurities in Cu. Nevertheless, it is seen from Table II that quantitative consistency with experiment is obtained already, albeit the magnitude of the wind valence of Al in Al metal seems to be too small, while Cu in Al metal is a factor of two too large. The calculated wind valences are seen to clearly dominate a possible direct valence contribution. Cu in Cu metal presents a remarkable case in that the experimentally observed negative effective valence cannot be explained on the basis of the initial position ($Z_{\text{wind}} > 0$) alone. Only after a proper calculation at the saddle point was performed, consistency with experiment is achieved.

IV. SUMMARY

It was shown how the electromigration wind force on a migrating atom anywhere along the path in an elementary step in lattice diffusion can be computed. The final expressions involve Brillouin-zone integrals that have to be evaluated for every different impurity cluster geometry. Corresponding expressions with respect to host lattice positions need to be evaluated only once. From these Brillouin-zone integrals, the matrix describing the backscattering of conduction electrons from the crys-

talline environment of the impurity cluster is obtained. A combination of multiple scattering in the crystal with electron scattering in the impurity cluster yields the alloy wave function, and matrix elements of the force operator can be evaluated at positions along the migration path.

The wind valence Z_{wind} was calculated for electromigrating Al and Cu atoms in Al and Cu metal, *both* at the initial position *and* at the point halfway along the migration path. Invariably the wind force was found to be largest at the saddle-point position. This reflects the maximum of the cross section for Bloch electron scattering of the migrating atom, since the deviation from the perfect lattice is largest at the saddle point. At the initial position (the migrating atom and the vacancy both at lattice sites) close agreement with a conventional, but limited approach was established. In spite of the fact that any perturbation of the surrounding lattice was neglected for the time being, qualitative agreement with experiment was readily demonstrated by averaging calculated wind valences over the migration path. Cu in Cu metal forms a remarkable example of a system where it is not sufficient to calculate Z_{wind} at the initial position in order to estimate the path-averaged wind valence: the sign of the wind valence calculated at the initial position is positive, whereas experiment dictates self-electromigration of Cu in a direction opposed to the electric field ($Z_{\text{wind}} < 0$). Only after accounting for the saddle-point position, was agreement with experiment achieved in this matter. Incorporation of the effects of local lattice deformation and charge transfer to neighboring atoms is expected to further improve the results of the wind force calculations. Once the implementation of a larger impurity cluster, including displaced atoms neighboring the migrating ion, is in place, a recently derived generalized Friedel sum rule[21] will be used to assure charge neutrality in the system. Electromigration of Al in Al metal in the presence of other atoms, effects of alloying through a rigid Fermi-level shift, and variations in the residual resistivity as a function of position, are topics that will be addressed. Furthermore, it should be possible to shed light on the direct force in these systems through comparison of experimental data on self-electromigration in metals with calculated wind valences.

ACKNOWLEDGMENT

Part of this work was performed under the auspices of the U.S. Department of Energy by Lawrence Livermore National Laboratory under Contract No. W-7405-ENG-48.

APPENDIX

For a spherically symmetric muffin-tin potential located at $\vec{R}_n$, the single-site t matrix is given by

$$t_{nl} = -\sin\eta_{nl}\, e^{i\eta_{nl}} \ . \tag{A1}$$

Quantities like the phase shifts η_{nl} do depend on energy, but this energy dependence has been suppressed.

For a collection of muffin-tin potentials, propagation from site n to site n' over all possible scattering paths in the cluster is described by the cluster t matrix,

$$\begin{aligned} T_{nLn'L'} &= \left[t\,(1-Bt)^{-1}\right]_{nLn'L'} \\ &= t_{nl}\delta_{nn'}\delta_{LL'} + t_{nl}B^{nn'}_{LL'}t_{n'l'} \\ &\quad + \sum_{n_1L_1} t_{nl}B^{nn_1}_{LL_1}t_{n_1l_1}B^{n_1n'}_{L_1L'}t_{n'l'} + \cdots \ , \end{aligned} \tag{A2}$$

where $\delta_{LL'}$ stands for $\delta_{ll'}\delta_{mm'}$. The free space structural Green function matrix at energy ϵ,

$$B^{nn'}_{LL'} = -4\pi\, i^{l-l'+1} \sum_{L''} C_{LL'L''}\, h^+_{l''}(\sqrt{\epsilon}\,\vec{R}_{nn'})Y_{L''}(\hat{R}_{nn'}) \ , \tag{A3}$$

is defined to vanish for $n = n'$,

$$B^{nn}_{LL'} \equiv 0 \ . \tag{A4}$$

In Eq. (A3) $C_{LL'L''} = \int \mathrm{d}\hat{x}\, Y_L(\hat{x})Y_{L'}(\hat{x})Y_{L''}(\hat{x})$ are Gaunt coefficients expressed in terms of real spherical harmonics $Y_L(\hat{x})$. Apparently, the vectorial matrix $\vec{D}_{LL'}$ differs a factor $\sqrt{\frac{3}{4\pi}}$ from the Gaunt coefficients for $l'' = 1$. The spherical Hankel function h^+_l is a linear combination of spherical Bessel (j_l) and Neumann functions [n_l, $h^+_l(x) = j_l(x) + in_l(x)$].

* Present address: Department of Physics, Tulane University, New Orleans, LA 70118.

[1] J. van Ek and A. Lodder, Defect Diffusion Forum **115-116**, 1 (1994).
[2] H.B. Huntington, in *Diffusion in Solids: Recent Developments*, edited by A.S. Nowick and J.J. Burton (Academic Press, New York, 1975), p. 303.
[3] P.S. Ho and T. Kwok, Rep. Prog. Phys. **52**, 301 (1989).
[4] R.S. Sorbello, A. Lodder, and S.J. Hoving, Phys. Rev. B **25**, 6178 (1982).
[5] M.G.E. Brand and A. Lodder, Phys. Status Solidi B **133**, 119 (1986).
[6] R.P. Gupta, Phys. Rev. B **25**, 5188 (1982); R.P. Gupta, Y. Serruys, G. Brebec, and Y. Adda, *ibid.* **27**, 672 (1983).
[7] J. van Ek and A. Lodder, J. Phys. Condens. Matter **3**, 8403 (1991).
[8] R.S. Sorbello, J. Phys. Chem. Solids **34**, 937 (1973); **42**, 309 (1981).
[9] A. Lodder, J. Phys. F **14**, 2943 (1984).
[10] A. Lodder, J. Phys. F **6**, 1885 (1976).
[11] P.M. Oppeneer and A. Lodder, J. Phys. F **17**, 1901 (1987).
[12] J. van Ek and A. Lodder, J. Phys. Condens. Matter **3**, 7331 (1991).
[13] J. van Ek and A. Lodder, J. Alloys Comp. **185**, 207 (1992).
[14] J. van Ek and A. Lodder, J. Phys. Condens. Matter **3**, 7363 (1991).
[15] $\vec{D}_{LL'} = \int d\hat{x}\, Y_L(\hat{x})\,\hat{x}\, Y_{L'}(\hat{x})$, with $Y_L(\hat{x})$ real spherical harmonics.
[16] N.A.W. Holtzwarth, Phys. Rev. B **11**, 3718 (1975).
[17] P.M. Oppeneer and A. Lodder, J. Phys. F **17**, 1885 (1987).
[18] J.P. Dekker and A. Lodder (unpublished).
[19] P.T. Coleridge, J. Molenaar, and A. Lodder, J. Phys. C. **15**, 6943 (1982).
[20] C. Bosvieux and J. Friedel, J. Phys. Chem. Solids **23**, 123 (1962).
[21] A. Lodder and J.P. Dekker, Phys. Rev. B **49**, 10 206 (1994).